Forschungszentrum Karlsruhe
in der Helmholtz-Gemeinschaft
Wissenschaftliche Berichte
FZKA 6860

Neutron Capture Resonances in ^{110}CD, ^{112}Cd, ^{114}Cd, and ^{116}Cd.

K. Wisshak, F. Voss, F. Käppeler
Institut für Kernphysik

Oktober 2003

FORSCHUNGSZENTRUM KARLSRUHE
in der Helmholtz-Gemeinschaft
Wissenschaftliche Berichte
FZKA 6860

NEUTRON CAPTURE RESONANCES IN ^{110}Cd,^{112}Cd,^{114}Cd, AND ^{116}Cd

K. WISSHAK, F. VOSS, and F. KÄPPELER

Institut für Kernphysik

Forschungszentrum Karlsruhe GmbH, Karlsruhe
2003

Impressum der Print-Ausgabe:

Als Manuskript gedruckt

Forschungszentrum Karlsruhe GmbH
Postfach 3640, 76021 Karlsruhe

Mitglied der Hermann von Helmholtz-Gemeinschaft
Deutscher Forschungszentren (HGF)

ISSN 0947-8620

ABSTRACT

The neutron capture cross sections of ^{110}Cd, ^{112}Cd, ^{114}Cd, and ^{116}Cd, which were determined recently with the Karlsruhe $4\pi BaF_2$ detector, have been reanalyzed at low energies. Resonance parameters were extracted by means of a shape analysis program, thus allowing a more reliable determination of the averaged cross sections below 10 keV. This study confirms the previously reported stellar cross sections. Accordingly, the results of the s–process studies based on these data remain unchanged.

ZUSAMMENFASSUNG

NEUTRONENEINFANGRESONANZEN IN ^{110}Cd, ^{112}Cd, ^{114}Cd UND ^{116}Cd

Die kürzlich mit dem Karlsruher $4\pi BaF_2$ Detektor gemessenen Neutroneneinfangquerschnitte von ^{110}Cd, ^{112}Cd, ^{114}Cd und ^{116}Cd wurden bei niedrigen Energien neu ausgewertet. Mit einem Analyseprogramm wurden Resonanzparameter ermittelt, die eine genauere Bestimmung der Querschnitte unterhalb von 10 keV ermöglichen. Die neuen Ergebnisse bestätigen die früher veröffentlichten stellaren Querschnitte. Daher bleiben die Untersuchungen zum s–Prozess, die auf diesen Daten basieren, unverändert gültig.

Contents

1 INTRODUCTION

The Karlsruhe 4π BaF_2 Detector [1] has been established for the purpose of improved and accurate measurements of neutron capture cross sections in the keV range that are required for a comprehensive study of the nucleosynthesis of heavy elements in the so called s-process [2]. The main advantage of the experimental setup is the high efficiency and good gamma-ray energy resolution which allows to register capture events with a probability of more than 95%. The neutron energy is determined by the time-of-flight (TOF) technique. The flight path used in the actual experiments, which was chosen to optimize the neutron flux at the sample position, is comparably short (79 cm) compared to other TOF-experiments. This has the consequence that the resolution in neutron energy is limited and resonances are not resolved in general. For the determination of stellar neutron capture cross sections this is not a significant complication, although some physical information is missing.

However, for isotopes with small cross sections and correspondingly low level densities isolated resonances can be observed in the neutron energy range between 3 and 20 keV. Of the 66 isotopes measured with this detector in more than a decade, resonance analyses could be performed only in six cases, for ^{136}Ba [3], ^{116,118,120}Sn [4], and ^{142,144}Nd [5]. As a practical application, summing the areas of the capture of the resonances provides an independent way of determining the average cross section at lower energies.

In the present case resolved resonances could be investigated for four isotopes for a series of the even isotopes ^{110,112,114,116}Cd. The results of the cross section measurements and the astrophysical consequences have already been published in Ref. [6]. A detailed description of the technical part, including data evaluation methods, calculation of correction factors, and the results of individual experimental runs, can be found in Ref. [7].

The data reported in Ref. [6] have been reanalysed by means of a shape analysis program. Of the 278 resonances, which were analyzed in the neutron energy range from 2.8 to 10 keV, only 16 previously reported resonances could not be identified, whereas 45 resonances are described for the first time. From the resonance parameters, more reliable values for the low energy part of the stellar cross sections were derived, an improvement, that is especially important, since stellar model calculations indicate that most of the s process takes place at thermal energies below 10 keV [8, 9].

2 EXPERIMENT AND DATA EVALUATION

Experiment and data analysis have been described in detail in Refs. [6, 7]. Continuous neutron spectra were produced via the ^{7}Li(p,n)^{7}Be reaction using the pulsed proton beam of the Karlsruhe 3.75 MV Van de Graaff accelerator. Capture events were registered with

Table 1: Parameters for calculating the neutron width according to equation (2)

	^{110}Cd	^{112}Cd	^{114}Cd	^{116}Cd
D_s(eV)	155	190	235	390
S_1 (10^{-4})	3.0	3.2	3.5	3.2
R (fm)[a]	6.468	6.507	6.546	6.584
		$(kR)^{2b}$		
2 keV	0.00405	0.00409	0.00414	0.00419
5 keV	0.01011	0.01024	0.01036	0.01048
10 keV	0.02023	0.02047	0.02072	0.02096
15 keV	0.03034	0.03071	0.03108	0.03144
		$g\Gamma_n$(meV)		
2 keV	8.38	11.09	15.18	23.30
5 keV	32.92	43.56	59.63	91.52
10 keV	92.19	121.97	166.94	256.20
15 keV	167.70	221.85	303.61	465.88

[a] Calculated as $R=1.35A^{1/3}$
[b] Calculated as $(kR)^2=(R/\lambda_c)^2\times 2E/mc^2$,
with E in eV, λ_c=0.21fm, $mc^2=9.38\text{x}10^8$eV

the Karlsruhe 4π BaF_2 detector [1] with a time resolution of about 1 ns. The samples, enriched to 95.5 % in ^{110}Cd, 97.9% in ^{112}Cd, 99.1% in ^{114}Cd, and 92.4 % in ^{116}Cd, were located at a neutron flight path of 79 cm. Sample masses ranged between 2.5 and 6.0 g. Three runs were performed with different maximum neutron energies and acquisition modes [6]. All spectra could be analysed down to a minimum energy of 2.8 keV.

After summation of the capture yields from the three runs, the resulting TOF-spectra were analysed with the FANAC code [10] in the same way as described for ^{136}Ba [3], ^{116,118,120}Sn [4], and $^{142.144}$Nd [5]. The global input parameters like strength functions or nuclear radii were taken from the calculations of the multiple scattering and self–shielding corrections described in Ref. [7]. Known neutron widths of s– and p–wave resonances as well as resonance spins were adopted from Ref. [11].

The TOF measurement of the neutron energy is determined by the pulse width of the proton beam (0.7 ns), the time resolution of the 4π BaF_2 detector (0.5 ns), and by the sample thickness of 1.7 - 4.0 mm, resulting in a limited resolution in neutron energy between 0.3 and 0.5% at energies of 3 keV and 10 keV, respectively. Within these uncertainties all resonance energies were found in agreement with the data listed in Ref. [11].

Since even the shape of broad s–wave resonances is to a large extent determined by the experimental resolution, it was not possible to derive the individual resonance parameters Γ_n or Γ_γ directly from the present experiment. Instead, the resonance areas $A_\gamma = g\Gamma_n\Gamma_\gamma/(\Gamma_n+\Gamma_\gamma)$ were determined in the fits. However, the neutron widths of most resonances are known [11] and could be used in the analysis.

Where no information on Γ_n was available, the average neutron width was calculated via the relation [12]

$$g_J < \Gamma_n >_{lJ} = \nu_{lJ} g_J D_J S_l \sqrt{E} v_l(E) \qquad (1)$$

where the quantities g, D, S, ν, and v_l denote the statistical weight factor, the mean level spacing, the strength function, the number of possible channel spins, and the penetrability factor. For p–wave resonances, this expression reduces to

$$g < \Gamma_n >_1 = D_s S_1 \sqrt{E} \frac{(kR)^2}{1 + (kR)^2}. \qquad (2)$$

The respective input data for this calculation and the results for $g\Gamma_n$ are given in Table 1.

The reliability of the resonance areas A_γ depends on the available experimental information on neutron widths and spins. For the individual cadmium isotopes the situation is more favorable compared to the previously studied barium and neodymium isotopes [3, 5]. This is important since unknown neutron widths of s–wave resonances give rise to systematic uncertainties if these resonances dominate the cross section. While this was problematic for barium and neodymium, which belong to a mass region with a local maximum of the s-wave strength function, cadmium is much less affected since it is situated close to a minimum of the s-wave strength function.

For s- and p–wave resonances there is good information on g and $g\Gamma_n$ for ^{110}Cd and ^{112}Cd, but the respective values are partly missing for ^{114}Cd and ^{116}Cd, especially above 7 keV. Missing values for $g\Gamma_n$ were calculated according to Eq.(2) and g=1 was arbitrarily assumed in these cases. Below 7 keV, 30% and 13% of these values had to be calculated for ^{110}Cd and ^{112}Cd, respectively. This fraction was considerably larger for ^{114}Cd and ^{116}Cd (58% and 69%, respectively). Thus systematic uncertainties due to missing neutron widths and g values can not be excluded, but are difficult to estimate. The resonance energies given in Ref. [11] are those of Liou et al. [13]. Musgrove et al. [14], who remeasured these resonances up 7 keV, found several new resonances, but reported a slightly different energy scale. When these data were included in Ref. [11], the energy calibration of Liou et al. [13] was adopted.

In the first step of the present analysis the energy of well isolated resonances was determined. Comparison with the data of Ref. [11] showed that the differences in resonance energy are smoothly increasing with energy. Therefore, this relation was used to adjust all resonance energies to the respective values of Ref. [11], which were then treated as fixed parameters in the fits. These resonance energies provided sufficiently good fits in most cases. Nevertheless, the resonances were also investigated individually, and the energy was modified if better agreement with the measured capture yield could be obtained.

As shown by Koehler et al. [15] for ^{116,120}Sn, the shift in energy scale for the resonances measured with the Karlsruhe $4\pi BaF_2$ detector is well compatible with the quoted flight path uncertainty. Accordingly, the corrected resonance energies are consistent with the data of Ref. [11]. The largest differences are observed for ^{110}Cd, where one finds differences of about 4 eV around 3 – 4 keV. These increase to 10 eV between 5 and 6 keV and to 20 eV in the energy range from 7 to 10 keV. For ^{112,114}Cd the agreement is even better, and it is almost perfect for ^{116}Cd in spite of the fact that this sample was nearly a factor of two thicker (4 mm) than the others. Among the very few exceptions are resonances in ^{114}Cd at 8.9460, 9.9583, and 10.088 keV, where the larger energy differences of up to 68 eV are due to the present assignment of a doublet structure.

In the second step, the areas A_γ of all resonances were determined. The p-wave resonances were analyzed assuming the two possible values for the statistical weight factor g=1 and g=2. Since the results of the two fits were in general very similar, the average was adopted, except in cases where g values are explicitely specified in Ref. [11]. The present resonance energies and areas are listed in Tables 2 to 5. The quoted statistical uncertainties are those provided by the FANAC code. The experimental capture yields and the FANAC fits are compared in Figs. 1 to 4.

There are six weak resonances in ^{110}Cd and ten in ^{112}Cd, which are quoted in Ref. [11] from the work of Musgrove et al. [14], but could not be identified in our data. None of these resonances was reported by Liou et al. [13] either. In total. 45 resonances were identified in the present experiment for the first time. However, all these resonances are located above 7 – 8 keV, at neutron energies that were not included in the analysis of Musgrove et al. [14].

The resonance areas, A_γ, quoted in Ref. [11] are the original data of Musgrove et al. [14]. The normalization of these data has later been revised [16], but the individual values changed only by about 2%. Compared with the present results there are obvious systematic differences correlated with the resonance strengths. Considering groups of strong (A_γ > 80 meV), weak (A_γ < 40 meV) and intermediate resonances, one finds the following picture. For ^{110}Cd strong resonances are about 70% enhanced, while weak and intermediate resonances agree on average within ∼10%. This enhancement of strong resonances reduces in ^{112}Cd to ∼30%, but for this isotope the weak resonances are smaller by ∼20%. In case of ^{114}Cd the strong resonances are still less enhanced (by 15% on average), whereas nearly perfect agreement is found for ^{116}Cd. For the last two isotopes the weak and intermediate resonances are in fair agreement, the remaining differences being compatible with statistical uncertainties and with the limited experimental energy resolution, which does not always allow to resolve multiplets.

The large discrepancy found for the strong resonances in ^{110}Cd might be correlated with the fact that – especially for this isotope – nearly all of them are s–wave resonances with comparably large neutron widths. The difficulties in analyzing s–wave resonances measured at long flight paths and using the pulse height weighting technique have been extensively discussed and are claimed to be solved [17, 18]. However, in these old data, problems with prompt neutron sensitivity or uncertain weighting functions may well persist, especially for resonances with hard capture γ–ray spectra. That the percentage of s–waves decreases with mass number may support the observed trend, in particular since almost all strong resonances in ^{116}Cd are p-waves.

These problems are not relevant in the present case. Due to the short primary flight-path, the additional TOF between sample and detector modules ensures that background from scattered neutrons can be discriminated and does not interfere with the respective resonance. The correction for prompt capture after scattering is known to be correctly treated by FANAC. Finally, the response of the nearly 100% efficient 4π detector is completely insensitive to variations in the capture γ–ray spectra of individual resonances.

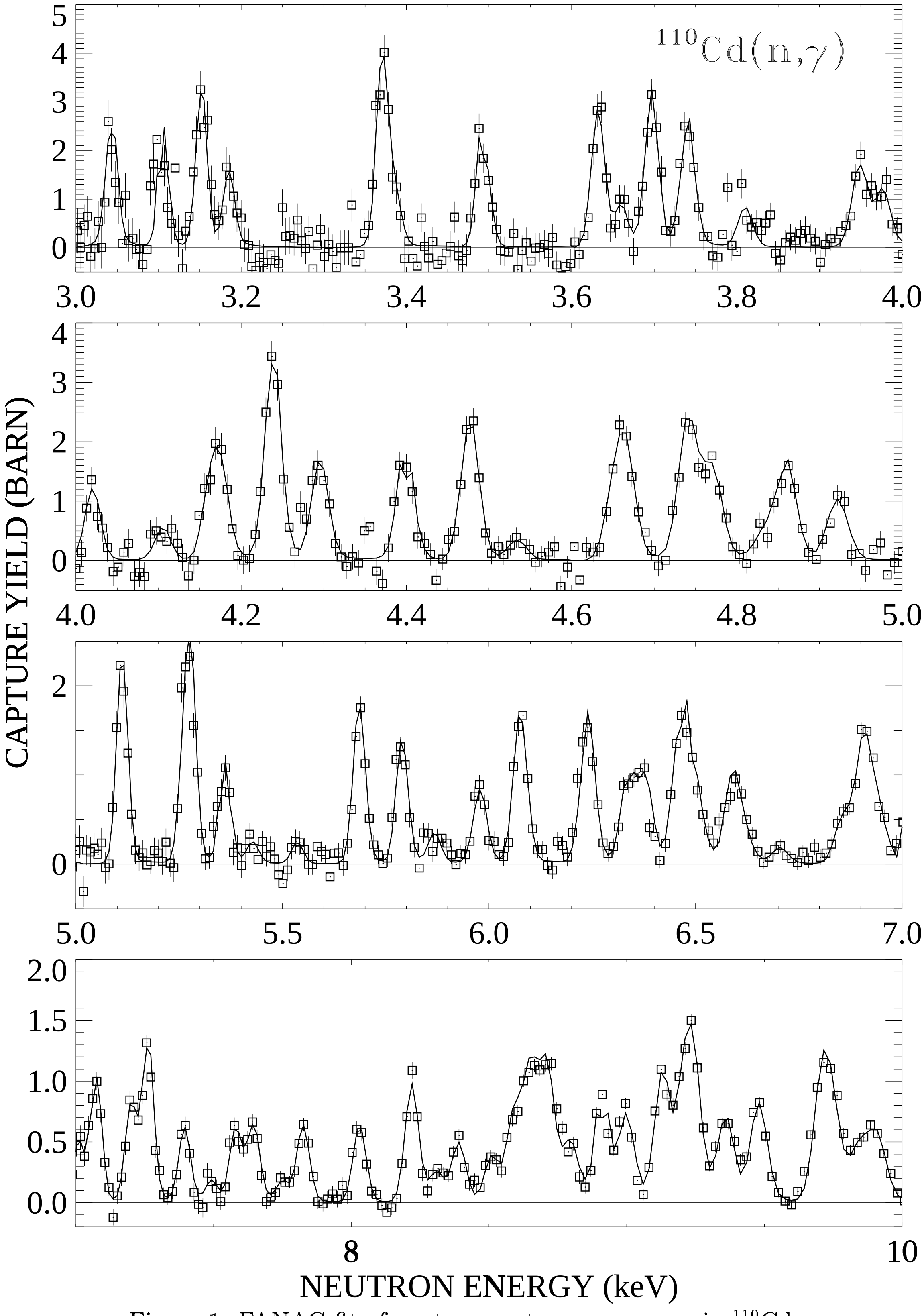

Figure 1: FANAC fit of neutron capture resonances in ^{110}Cd.

Table 2: Parameters of capture resonances in ^{110}Cd

Resonance energy Ref.[11] (keV)	Resonance energy This Work (keV)	g	l	$g\Gamma_n$[1] (meV)	A_γ[4] This Work (meV)	ΔA_γ This Work (meV)	A_γ Ref.[11] (meV)
3.0422	3.043		0	1500	84.9	13.1	
3.1057	3.106		0	134	36.4	5.4	44
3.1531	3.152	2	1	74	45.8	3.4	73
3.1837	3.185		1	22	21.6	1.6	27
3.3751	3.371[2]		0	220	112.0	4.9	71
3.380	3.387[2]			22[3]	12.0	2.8	26
3.4964	3.493		0	95	51.6	3.4	46
3.6364	3.632	2	1	110	56.9	3.9	71
3.6678	3.660		1	67	16.6	3.4	13
3.7021	3.697		0	103	81.9	2.0	72
3.7444	3.741		0	500	92.8	6.4	72
3.8044	3.810		1	25	16.4	2.6	21
3.842							5
3.9535	3.949		0	1000	80.0	7.4	64
3.9809	3.977		1	28	26.7	3.2	19
4.030	4.020			30[3]	27.7	2.5	18
4.0990	4.105		1	56	13.6	3.3	12
4.1615	4.163[2]		1	47	31.5	3.8	24
4.1807	4.177[2]		1	110	32.4	5.3	42
4.2428	4.239		0	330	143.2	5.3	113
4.3048	4.295		0	140	88.3	3.5	47
4.4023	4.399		0	340	89.8	6.5	57
4.4800	4.477		1	105	73.8	3.7	83
4.519							5
4.543	4.534			30[3]	9.8	3.0	9
4.6611	4.652[2]		1	76	42.5	5.4	53
4.6751	4.667[2]		1	92	48.4	4.7	39
4.7477	4.740		0	145	111.3	1.9	87
4.779	4.770			35[3]	55.1	3.6	53
4.840	4.833[2]			35[3]	11.7	4.9	12
4.8645	4.859[2]		0	60	56.4	5.0	63
4.929	4.922			35[3]	40.3	5.7	32
4.980							8
5.112	5.102[2]			40[3]	9.9	5.2	34
5.1214	5.113[2]		0	720	156.5	20.2	66
5.276	5.260[2]			40[3]	33.6	3.6	71
5.2910	5.278[2]		0	540	152.8	9.6	55
5.3699	5.361		0	160	78.7	6.8	69
5.438	5.428			40[3]	10.4	4.1	15
5.546	5.536			40[3]	11.6	4.2	12
5.606							5

Table 2 (continued)

Resonance energy Ref.[11] (keV)	Resonance energy This Work (keV)	g	l	$g\Gamma_n$[1] (meV)	A_γ[4] This Work (meV)	ΔA_γ This Work (meV)	A_γ Ref.[11] (meV)
5.6942	5,686		0	310	152.5	20.3	83
5.707							34
5.8028	5.790		0	190	104.3	5.2	54
5.805							31
5.872	5.868			40[3]	18.5	4.2	11
5.9837	5.979		0	1300	84.2	17.9	57
6.0890	6.076		0	810	169.3	13.7	131
6.241	6.231[2]			60[3]	42.3	5.5	75
6.2590	6.246[2]		0	230	56.6	6.3	51
6.3439	6.337[2]		0	540	117.4	15.0	69
6.389	6.379[2]			70[3]	66.9	9.6	56
6.4689	6.459[2]	2	1	200	89.2	9.5	75
6.4874	6.485[2]		0	180	57.7	5.4	58
6.512	6.512			50[3]	20.4	4.3	61
6.6019	6.590		0	390	127.3	12.9	58
6.632	6.622			50[3]	21.7	8.1	35
6.730	6.705			50[3]	13.1	4.6	9
6.867	6.857			50[3]	41.6	4.1	35
6.9137	6.908		0	1000	188.3	14.5	90
6.9373	6.947	1	1	240	36.4	7.2	74
	7.010			70[3]	43.6	4.5	
7.0836	7.072		0	330	94.3	11.0	
	7.200			70[3]	73.4	4.3	
7.2768	7.260		0	280	176.8	12.6	
	7.395			75[3]	59.8	4.4	
	7.493			80[3]	16.3	3.9	
	7.580			80[3]	63.5	4.2	
7.6694	7.645		0	1100	104.1	10.7	
	7.750			80[3]	18.4	3.3	
	7.825			85[3]	71.1	3.8	
	8.030			85[3]	76.3	10.7	
	8.220			90[3]	125.7	12.3	
	8.310			90[3]	31.2	9.2	
	8.390			90[3]	65.0	9.5	
	8.510			95[3]	52.4	10.0	
	8.590			95[3]	97.7	10.7	

Table 2 (continued)

Resonance energy Ref.[11] (keV)	This Work (keV)	g	l	$g\Gamma_n$[1] (meV)	A_γ[4] This Work (meV)	ΔA_γ (meV)	A_γ Ref.[11] (meV)
	8.650			95[3]	145.9	7.7	
8.7188	8.710		0	1300	221.5	15.3	
8.8222	8.797		0	2800	97.5	17.7	
8.9345	8.910		0	530	174.4	12.7	
9.0254	9.000		0	510	177.4	12.1	
9.1463	9.131		0	1000	242.4	79.0	
9.2210	9.210		0	920	113.9	79.0	
9.2502	9.225		0	1000	90.9	79.0	
9.2697	9.244		0	1700	179.0	79.0	
	9.360			105[3]	121.2	11.4	
	9.480			110[3]	146.7	11.7	
	9.710			110[3]	184.7	12.7	
	9.750			110[3]	109.7	13.0	
	9.910			120[3]	103.9	11.1	
9.8600	9.845		0	2300	115.9	79.0	

[1]The values for g, l, and $g\Gamma_n$ were taken from Ref. [11].
[2]Unresolved doublets.
[3]Calculated according to equation (2).
[4]$A_\gamma = g\Gamma_n\Gamma_\gamma/(\Gamma_n + \Gamma_\gamma)$.

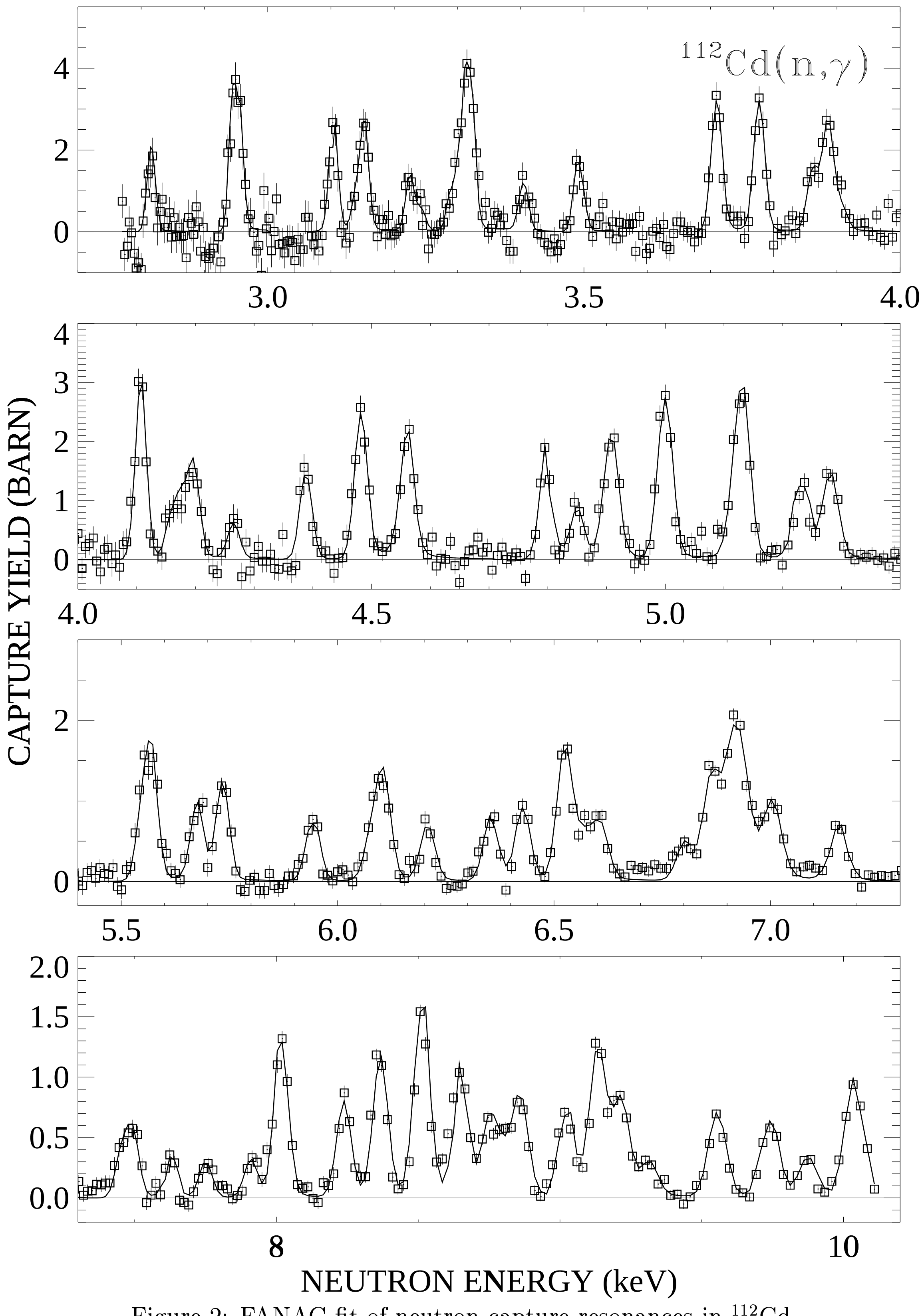

Figure 2: FANAC fit of neutron capture resonances in ^{112}Cd.

Table 3: Parameters of capture resonances in ^{112}Cd

Resonance energy Ref.[11] (keV)	This Work (keV)	g	l	$g\Gamma_n$[1] (meV)	A_γ[4] This Work (meV)	ΔA_γ This Work (meV)	A_γ Ref.[11] (meV)
2.8134	2.813[2]		1	19	11.8	4.5	
2.8175	2.818[2]		1	19	12.0	5.3	37
2.943	2.945[2]			56	39.1	8.4	33
2.9515	2.957[2]		0	230	59.4	6.4	62
3.0058			1	21			
3.1038	3.104		0	490	79.6	7.4	73
3.139	3.139[2]			22[3]	10.2	2.4	11
3.1536	3.153[2]	2	1	105	38.8	3.0	58
3.2247	3.225[2]		1	47	19.6	2.5	19
3.243	3.243[2]			24[3]	6.5	2.0	5
3.2898	3.290[2]		1	46	13.4	2.3	21
3.3069	3.307[2]		0	155	58.9	4.4	53
3.3205	3.321[2]	2	1	140	57.7	2.8	71
3.4043	3.404		1	25	18.5	2.0	26
3.4919	3.492		0	140	63.1	7.9	53
3.7101	3.710		1	47	69.1	6.1	28
3.713							50
3.7766	3.777	2	1	220	75.1	3.8	116
3.8619	3.862[2]		1	55	33.0	2.7	38
3.8857	3.886[2]	2	1	69	59.8	2.7	71
3.907	3.907[2]			30[3]	14.0	2.5	20
4.089							10
4.1069	4.107	2	1	210	83.3	4.4	90
4.1527	4.158[2]		1	34	17.6	2.7	18
4.180	4.176[2]			35[3]	22.7	4.0	20
4.2000	4.197[2]		0	100	75.0	4.9	45
4.2633	4.265		1	46	16.8	4.7	17
4.3927	4.388		1	91	44.7	4.4	54
4.477							35
4.4867	4.482	2	1	97	76.9	3.4	74
4.519							7
4.5583	4.561		0	1700	134.5	14.9	79
4.571							52
4.7983	4.798		0	125	55.3	7.9	55
4.8543	4.850	1	1	92	31.1	4.7	47
4.9075	4.908		0	940	136.0	18.1	77
4.918							32
5.0011	5.000	2	1	240	117.5	5.9	113
5.117	5.112[2]			45	17.4	4.2	29
5.1365	5.131[2]	2	1	210	116.2	5.1	113
5.2366	5.232		0	160	53.3	7.1	59
5.2858	5.281	2	1	91	65.2	4.0	78
5.433							6

Table 3 (continued)

Resonance energy Ref.[11] (keV)	This Work (keV)	g	l	$g\Gamma_n$ [1] (meV)	A_γ [4] This Work (meV)	ΔA_γ (meV)	A_γ Ref.[11] (meV)
5.5522	5.547[2]	2	1	88	39.0	4.3	55
5.5749	5.570[2]		0	750	127.1	13.0	71
5.587							30
5.673							10
5.6860	5.676		0	950	85.5	15.8	76
5.7344	5.734	2	1	93	67.0	3.6	50
5.750							36
5.9483	5.943		0	620	80.1	13.8	63
6.0851	6.080[2]		0	1600	65.2	12.7	68
6.1124	6.107[2]	2	1	160	69.2	4.0	81
6.218	6.208			60[3]	42.9	4.6	42
6.3591	6.354		0	520	94.8	22.8	60
6.4334	6.428	2	1	210	68.7	6.9	95
6.5291	6.525	2	1	320	131.8	7.4	144
6.5770	6.572[2]		0	2400	58.5	5.2	81
6.618	6.608[2]			65[3]	51.0	6.1	62
6.808	6.803			70[3]	38.6	6.4	42
6.8745	6.864[2]	2	1	140	117.2	6.9	138
6.9200	6.910[2]	2	1	390	123.2	10.4	129
6.9373	6.937[2]	1	1	220	95.3	9.6	83
6.9755	7.005		0	2900	130.8	11.8	82
7.1676	7.157		0	400	76.1	6.9	
	7.453[2]			80[3]	36.2	14.5	
	7.493[2]			80[3]	54.7	12.9	
7.6400	7.630		0	170	25.5	16.6	
	7.750			80[3]	32.9	10.8	
	7.910			85[3]	36.6	12.6	
8.0075	8.000[2]		0	440	40.8	37.3	
8.0292	8.019[2]		0	480	183.5	51.9	
8.2483	8.238		0	1600	150.4	38.4	
8.3770	8.367		0	730	222.0	27.1	
8.5194	8.509[2]		0	540	245.5	31.9	
8.5367	8.527[2]		0	760	75.6	23.5	
8.6655	8.650		0	350	127.3	11.6	
	8.750[2]			95[3]	86.7	13.9	
	8.800[2]			95[2]	50.8	7.0	
	8.860			100[3]	129.3	15.8	
9.0419	9.022		0	400	177.8	13.5	
9.1535	9.134		0	2000	289.9	22.0	
9.2259	9.216		0	550	198.3	16.7	

Table 3 (continued)

Resonance energy Ref.[11] (keV)	This Work (keV)	g	l	$g\Gamma_n$[1] (meV)	A_γ[4] This Work (meV)	ΔA_γ (meV)	A_γ Ref.[11] (meV)
	9.315			110[3]	45.3	6.6	
9.5701	9.555		0	1100	172.8	17.1	
9.7389	9.738		0	370	165.7	12.1	
	9.875			110[3]	64.0	7.1	
10.043	10.040		0	630	233.9	15.4	

[1]The values for g, l, and $g\Gamma_n$ were taken from Ref. [11].
[2]Unresolved doublets.
[3]Calculated according to eq.(2).
[4]$A_\gamma = g\Gamma_n\Gamma_\gamma/(\Gamma_n + \Gamma_\gamma)$.

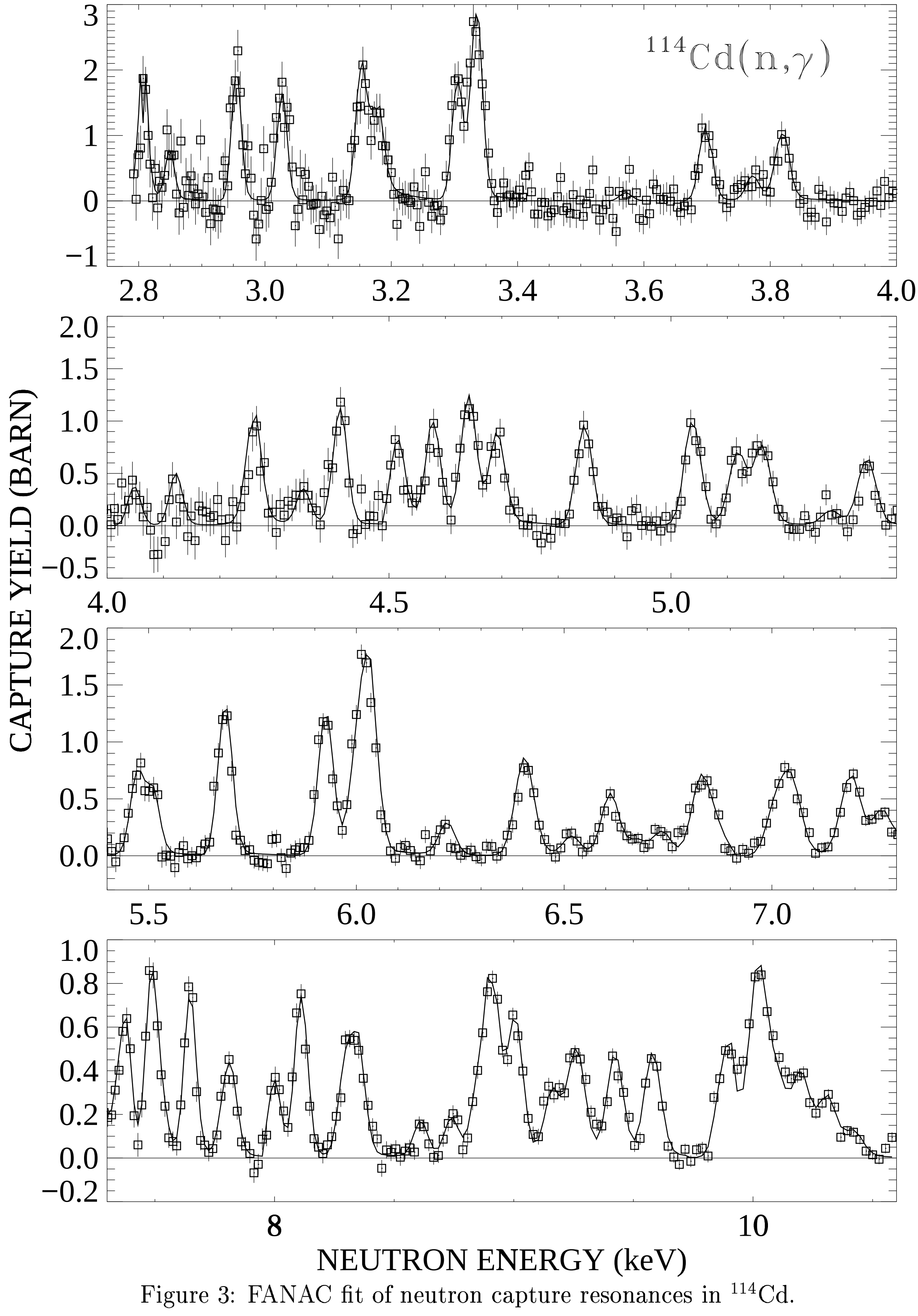

Figure 3: FANAC fit of neutron capture resonances in ^{114}Cd.

Table 4: Parameters of capture resonances in ^{114}Cd

Resonance energy Ref.[11] (keV)	Resonance energy This Work (keV)	g	l	$g\Gamma_n$[1] (meV)	A_γ[4] This Work (meV)	ΔA_γ This Work (meV)	A_γ Ref.[11] (meV)
2.8040	2.807		0	349	76.5	13.2	44
2.8493	2.849		1	40	10.9	2.5	22
2.9556	2.955		1	61	32.5	2.7	40
3.0271	3.027		1	49	28.0	2.7	34
3.155	3,152			30[3]	28.7	2.4	33
3.1780	3.178		0	3400	78.2	13.3	57
3.3054	3.305		1	86	39.0	3.1	44
3.3334	3.335	2	1	330	84.7	4.8	97
3.571	3.571			35[3]	3.2	2.5	3
3.6984	3.698		0	53	42.9	1.9	35
3.772	3.772			40[3]	9.2	2.5	11
3.8195	3.819		0	970	67.0	13.8	55
4.053	4.048			40[3]	11.2	2.4	15
4.132	4.122			40[3]	14.2	4.7	4
4.2580	4.260		0	2100	90.9	19.9	61
4.348	4.348			50[3]	11.8	2.6	18
4.4184	4.413	1	1	120	45.8	3.0	48
4.515	4.515[2]			50[3]	31.5	3.4	30
4.540	4.540[2]			50[3]	1.9	2.1	10
4.5828	4.578		0	260	84.4	14.0	43
4.6455	4.641	2	1	190	55.3	3.2	66
4.6918	4.692		0	320	75.6	12.6	43
4.856	4.846			60[3]	41.7	3.4	57
5.046	5.038			60[3]	47.8	3.2	38
5.128	5.118[2]			60[3]	34.1	3.3	36
5.171	5.161[2]			60[3]	39.7	3.4	43
5.294	5.284			65[3]	7.1	3.4	7
5.3570	5.347		0	430	63.9	19.0	46
5.482	5.472[2]			70[3]	41.8	3.1	42
5.5150	5.510[2]		0	680	62.6	15.3	47
5.689	5.684	2	1	70[3]	94.7	10.7	101
5.931	5.926	2	1	75[3]	92.6	8.1	105
6.017	6.002[2]			80[3]	72.7	7.8	69
6.0424	6.032[2]	2	1	580	137.4	7.0	136
6.223	6.218			80[3]	24.2	7.5	12
6.4066	6.397[2]		0	770	79.8	34.7	44
6.428	6.414[2]			85[3]	29.9	6.5	41
6.543	6.518			90[3]	16.3	7.8	11
6.620	6.611			90[3]	46.5	7.4	34
6.675	6.675			90[3]	11.7	6.8	16
6.745	6.735			95[3]	17.8	6.7	17
6.828	6.828[2]			95[3]	64.3	8.2	38
6.865	6.865[2]			95[3]	16.9	6.2	60

Table 4 (continued)

Resonance energy Ref.[11] (keV)	This Work (keV)	g	l	$g\Gamma_n$ [1] (meV)	A_γ [4] This Work (meV)	ΔA_γ (meV)	A_γ Ref.[11] (meV)
7.030	7.010[2]			100[3]	44.4	4.6	50
7.068	7.048[2]			100[3]	61.5	4.2	69
7.2026	7.190	2	1	1200	112.4	5.6	174
7.280	7.265			110[3]	41.0	3.7	41
7.358	7.338[2]			110[3]	21.6	3.4	28
7,3938	7.379[2]	1	1	420	73.4	5.1	69
7.4958	7.486[2]	2	1	1200	147.4	7.5	134
7.548	7.533[2]			115[3]	19.0	3.4	27
7.6620	7.647	2	1	490	107.7	4.7	132
7.813	7.788[2]			120[3]	21.4	3.1	35
7.8376	7.820[2]		0	1600	76.2	11.4	50
	8.000			120[3]	50.6	11.7	
	8.111			120[3]	105.0	8.3	
	8.295[2]			130[3]	58.7	10.4	
8.3686	8.350[2]		0	1400	123.1	37.7	
	8.611			130[3]	26.0	12.7	
	8.740			140[3]	31.1	11.3	
	8.850[2]			140[3]	48.0	11.5	
8.9460	8.910[2]		0	880	236.3	34.7	
	9.006			150[3]	115.4	5.9	
	9.160			150[3]	55.2	6.1	
9.2624	9.262		0	7800	166.4	42.3	
	9.423			160[3]	94.6	6.7	
	9.585			160[3]	96.9	5.2	
9.9583	9.890		0	950	183.9	33.1	
10.088	10.020		0	1300	293.5	31.7	
	10.100[2]			170[3]	81.5	8.8	
	10.200[2]			170[3]	86.9	10.4	
	10.310[2]			170[3]	63.7	11.2	
	10.420[2]			180[3]	26.1	9.6	

[1]The values for g, l, and $g\Gamma_n$ were taken from Ref. [11].
[2]Unresolved doublets.
[3]Calculated according to eq.(2).
[4]$A_\gamma = g\Gamma_n\Gamma_\gamma/(\Gamma_n + \Gamma_\gamma)$.

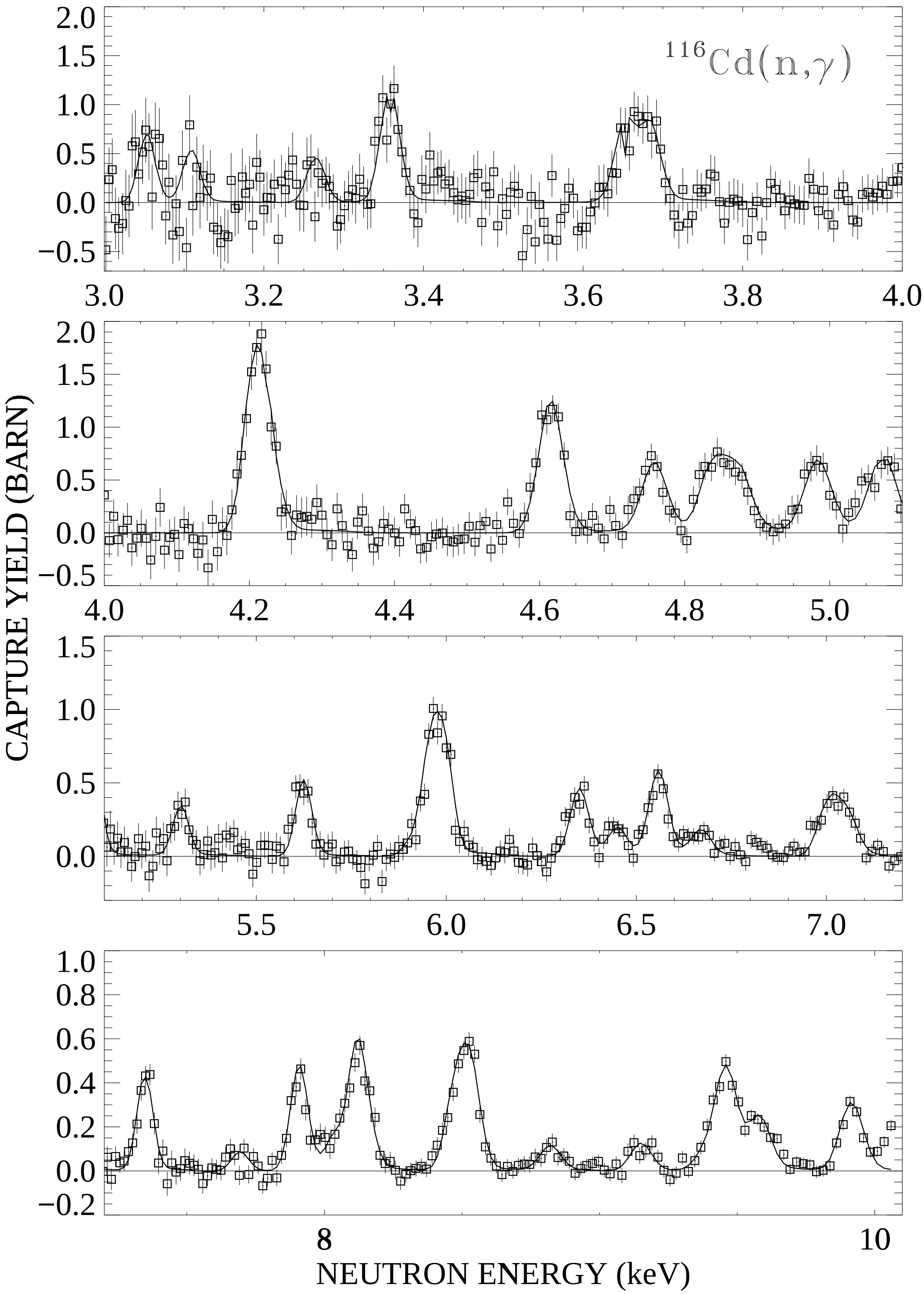

Figure 4: FANAC fit of neutron capture resonances in ^{116}Cd.

Table 5: Parameters of capture resonances in ^{116}Cd

Resonance energy Ref.[11] (keV)	Resonance energy This Work (keV)	g	l	$g\Gamma_n$[1] (meV)	A_γ[4] This Work (meV)	ΔA_γ This Work (meV)	A_γ Ref.[11] (meV)
3.053	3.053			45[3]	15.1	2.9	20
3.109	3.109			50[3]	11.8	3.0	10
3.265	3.265			50[3]	11.8	3.0	15
3.3580	3.358		0	240	75.4	6.6	51
3.6526	3.653[2]		0	670	70.7	9.8	47
3.684	3.684[2]			60[3]	24.7	2.9	32
4.2067	4.207[2]	2	1	140	83.0	4.2	65
4.228	4.228[2]			75[3]	15.1	2.6	39
4.6153	4.615	2	1	170	73.7	3.1	80
4.758	4.758			90[3]	37.2	2.9	50
4.843	4.838[2]			90[3]	38.2	3.7	48
4.8738	4.874[2]		0	750	73.1	15.6	41
4.983	4.983			95[3]	40.9	3.8	40
5.0725	5.073	1	1	640	69.5	5.9	82
5.3005	5.301		0	1600	57.8	15.8	36
5.624	5.624	2	1	115[3]	41.8	3.0	74
5.909	5.909[2]			125[3]	7.5	4.3	11
5.957	5.957[2]			130[3]	63.2	4.5	59
5.995	5.995[2]	2	1	130[3]	63.5	4.2	110
6.350	6.350			140[3]	48.0	3.7	55
6.455	6.450			140[3]	20.5	3.3	19
6.558	6.558			145[3]	63.7	4.1	77
6.670	6.670			145[3]	19.5	3.1	15
7.005	7.005[2]			160[3]	45.4	4.7	28
7.055	7.055[2]			160[3]	33.9	4.2	66
7.3471	7.347	2	1	1500	107.7	5.9	144
7.693	7.693			180[3]	15.1	4.4	15
7.913	7.908	2	1	190[3]	80.6	4.4	100
8.030	8.035[2]			190[3]	27.4	3.8	24
8.123	8.118[2]			195[3]	92.4	5.5	58
8.163	8.163[2]			195[3]	23.4	5.9	65
8.478	8.473[2]			210[3]	62.5	6.2	40
8.530	8.530[2]	2	1	210[3]	102.4	9.2	97
8.560	8.555[2]			210[3]	3.0	4.3	30
8.8222	8.822		0	3600	44.4	17.2	44
	9.150			230[3]	29.6	8.6	
	9.385[2]			240[3]	21.8	7.7	
	9.460[2]			240[3]	116.4	8.4	
	9.580			245[3]	60.0	7.0	
	9.915			255[3]	88.6	7.9	

Table 5 (continued)

Resonance energy		g	l	$g\Gamma_n$ [1]	A_γ [4]	ΔA_γ	A_γ
Ref.[11]	This Work				This Work		Ref.[11]
(keV)	(keV)			(meV)	(meV)	(meV)	(meV)

[1]The values for g, l, and $g\Gamma_n$ were taken from Ref. [11].
[2]Unresolved doublets.
[3]Calculated according to eq.(2).
[4]$A_\gamma = g\Gamma_n\Gamma_\gamma/(\Gamma_n + \Gamma_\gamma)$.

3 RESULTS

From the resonance parameters listed in Tables 2 to 5 averaged capture cross sections were calculated. The results are listed in Table 6 for the same energy bins that were used in our first evaluation [6]. For easier comparison the mean values for the entire energy range 3 to 10 keV are included as well. Obviously, the results obtained via resonance analysis differ not significantly from those of the analysis based on energy-averaged capture yields, as it was the case in our studies on ^{136}Ba [3], ^{116,118,120}Sn [4], and ^{142,144}Nd [5]. All previous examples, however, are characterized by comparably small capture cross sections with typical stellar averages at kT=30 keV between 35 and 100 mbarn, thus indicating large mean level spacings of 370 to 1610 eV for s-waves. Hence, agreement within the statistical uncertainties was obtained in these cases, confirming the proper treatment of the background due to scattered neutrons.

In the present experiment, only ^{116}Cd exhibits a similarly small stellar cross section, reflecting a large mean level spacing. Correspondongly, the two analyses are also in good agreement. The three other cadmium isotopes have significantly larger cross sections (130 to 240 mb) and lower mean level spacings (150 to 240 eV). As can be seen from Table 6 even for these isotopes the two evaluations agree within $\pm 2\sigma$ in nearly all energy intervals. The averages over the entire energy interval from 3 to 10 keV show that the new values are systematically higher by ~9% for the three lighter isotopes, nevertheless. A carefull look at the table shows in addition that in the neutron energy bin from 7.5 to 10 keV the statistical uncertainty of the new evaluation is about a factor of three larger for these three isotopes, too. This discrepancy can be explained by the fact that no information on the location of possible resonances was available at these energies. Thus, it was only possible to estimate the resonance energies from the observed structures in the cross sections. The limited resolution in neutron energy caused that certainly many resonances were overlooked in this way and consequently the quality of the fits was reduced. In the FANAC code [10] an error adjustment factor is defined which increases the statistical uncertainty if the fit is not perfect. In case of ^{116}Cd, where the resonances were known up to 8.8 keV, this problem does not show up and a much better agreement is found for the uncertainty in both evaluations.

Table 6: Averaged capture cross sections of ^{110}Cd, ^{112}Cd, ^{114}Cd, and ^{116}Cd.

Neutron energy (keV)	Capture cross section (mb)[1] This Work	Ref.[6]	This Work	Ref.[6]
	^{110}Cd		^{112}Cd	
3–5	846.8 ± 15.0	801.5 ± 29.7	691.8 ± 15.6	662.0 ± 24.5
5–7.5	624.3 ± 15.2	541.7 ± 11.9	548.6 ± 13.3	498.2 ± 10.5
7.5–10	548.2 ± 32.9	550.7 ± 8.8	478.2 ± 20.5	423.6 ± 7.2
3–10	660.7	619.1	564.4	518.4
	^{114}Cd		^{116}Cd	
3–5	449.1 ± 18.5	349.5 ± 19.6	289.4 ± 11.0	250.0 ± 20.8
5–7.5	398.1 ± 14.2	373.8 ± 9.0	172.8 ± 6.4	168.1 ± 8.7
7.5–10	306.8 ± 15.1	306.8 ± 5.8	145.9 ± 5.5	157.1 ± 5.5
3–10	380.1	342.9	196.5	187.6

[1]Including statistical uncertainties

Table 7: Maxwellian averaged neutron capture cross sections of ^{110}Cd, ^{112}Cd, ^{114}Cd, and ^{116}Cd.

Thermal energy (keV)	$<\sigma v>/v_T$ (mb)[1] This Work	Ref.[6]	This Work	Ref.[6]
	^{110}Cd		^{112}Cd	
8	527 ± 6	513 ± 6	435.5 ± 5.2	419.5 ± 5.2
10	466 ± 5	456 ± 5	381.2 ± 4.2	369.0 ± 4.2
15	366.6 ± 3.1	361.1 ± 3.1	295.3 ± 2.8	288.4 ± 2.8
20	306.8 ± 2.5	303.4 ± 2.5	245.4 ± 2.2	241.0 ± 2.2
25	266.7 ± 2.2	264.4 ± 2.2	212.8 ± 1.9	209.8 ± 1.9
30	238.2 ± 1.9	236.5 ± 1.9	190.1 ± 1.7	187.9 ± 1.7
	^{114}Cd		^{116}Cd	
8	297.4 ± 4.0	285.8 ± 4.0	161.5 ± 3.1	159.0 ± 3.1
10	259.8 ± 3.2	251.5 ± 3.2	142.8 ± 2.5	141.1 ± 2.5
15	201.4 ± 2.2	197.1 ± 2.2	112.9 ± 1.6	112.1 ± 1.6
20	167.7 ± 1.7	165.1 ± 1.7	95.0 ± 1.3	94.6 ± 1.3
25	145.8 ± 1.4	144.0 ± 1.4	83.2 ± 1.1	82.9 ± 1.1
30	130.5 ± 1.3	129.2 ± 1.3	75.0 ± 0.9	74.8 ± 0.9

[1]The 1.5% systematic uncertainty of the gold cross section is not included in the quoted uncertainties.

Based on the results of Table 6 revised Maxwellian averaged cross sections for thermal energies from $kT = 8$ to 30 keV are given in Table 7 together with the results of our first evaluation [6]. This comparison shows that the differences in the differential data have a comparably small impact on the stellar averages, all changes lying well within the quoted uncertainties. This holds even at $kT = 8$ keV where the influence of the new data is strongest. For the important s-only isotope ^{110}Cd, which has the largest cross section among the investigated cadmium isotopes, the stellar average at $kT = 8$ keV changed by less than 3%.

4 CONCLUSIONS

In total, 278 resonances in the neutron capture cross sections of the even-even cadmium isotopes were analyzed in the energy range from 2.8 to 10 keV. Compared to literature, 16 resonances could not be identified, but 45 were described for the first time. The cross section averages over the investigated energy range derived from the resonance areas agree with a first analysis based on energy-averaged cross sections only for ^{116}Cd, but are systematically larger by ~9% for the three other isotopes. This trend indicates that the limited TOF resolution of the of the investigated experiment starts to affect the resonance analysis at mean level spacings below ≈200 eV. The good agreement for ^{116}Cd confirms the reliability of background subtraction in experiments with the Karlsruhe 4π BaF_2 detector and the correct treatment of multiple scattering effects in both analyses. The Maxwellian averaged cross sections are essentially unchanged, at least for the important s-only isotope ^{110}Cd. Therefore, our previous s–process studies based on these cross sections remain valid [6].

5 ACKNOWLEDGMENTS

The help of F.H. Fröhner in using the FANAC code is gratefully appreciated.

References

[1] K. Wisshak, K. Guber, F. Käppeler, J. Krisch, H. Müller, G. Rupp, and F. Voss, Nucl. Instrum. Methods Phys. Res. A **292**, 595 (1990).

[2] F. Käppeler, H. Beer, and K. Wisshak, Rep. Prog. Phys. **52**, 945 (1989).

[3] F. Voss, K. Wisshak, and F. Käppeler, Phys. Rev. C **52**, 1102 (1995).

[4] K. Wisshak, F. Voss, and F. Käppeler, Phys. Rev. C **54**, 2732 (1996).

[5] K. Wisshak, F. Voss, and F. Käppeler, Phys. Rev. C **57**, 3452 (1998).

[6] K. Wisshak, F. Voss, F. Käppeler, and L. Kazakov, Phys. Rev. C **66**, 025801 (2002).

[7] K. Wisshak, F. Voss, F. Käppeler, and L. Kazakov, report FZKA–6619, Forschungszentrum Karlsruhe (2001)

[8] F. Käppeler, R. Gallino, M. Busso, G. Picchio, and C. Raiteri, Astrophys. J. **354**, 630 (1990).

[9] O. Straniero, R. Gallino, M. Busso, A. Chieffi, C. Raiteri, M. Limongi, and M. Salaris, Astrophys. J. **440**, L85 (1995).

[10] F. H. Fröhner, report KfK–2145, Kernforschungszentrum Karlsruhe (1977).

[11] S.I. Sukhoruchkin, Z.N. Soroko, and V.V. Deriglazov, Landolt-Börnstein, Numerical Data and Functional Relationships in Science and Technology, New Series, Group I, Vol 16, Subvolume B. Springer Berlin, Heidelberg, New York 1998.

[12] F.H. Fröhner, report GA–8380, Gulf General Atomic, 1968.

[13] H.I. Liou, G. Hacken, F. Rahn, J. Rainwater, M. Slagowitz, and W. Makofske, Phys. Rev. C **10**, 709 (1974).

[14] A.R. de L. Musgrove, B.J. Allen, and R.L. Macklin, J. Phys. G **4**, 771 (1978).

[15] P.E. Koehler, J.A. Harvey, R.R. Winters, K.H. Guber, and R.R. Spencer, Phys. Rev. C **64**, 065802 (2001).

[16] B. Allen, J. Boldeman, and R.R. Macklin, Nucl. Sci. Eng.**82**, 230 (1982).

[17] J.L. Tain, F. Gunsing, D. Cano-Ott *et al.* , Proc. Int. Conf. on Nuclear Data for Science and Technology, Tsukuba, Japan, October 7-12, 2001, J. of Nucl. Sci. and Techn. Supplement 2 August 2002.

[18] U. Abbondanno *et al.* , Nucl. Instrum. Methods Phys. Res. A, submitted May 2003.